

Journal of Solar Energy Research (JSER)

Journal homepage: www.jser.ut.ac.ir



Augmentation of Solar Air Heater Performance by Experimental Modification

Ibrahim S. Resen^{a,} Osamah Raad Skheel^b, Mudhar A. Al-Obaidi^b, Sura S. Al-Musawi^c, Ameera Hydrose^d

ARTICLE INFO

Article Type:

Received:2025.09.20 Accepted in revised form:2025.10.13

Keywords:

Thermal performance; Solar air heaters (SAHs); Rectangular Pipes; Effective absorption plate; Experimental study

ABSTRACT

The current research intends to create an efficient absorber plate aimed at enhancing energy capture through the use of an expanded absorber surface. To achieve this, an array of rectangular pipes is used to expand the absorber area. The investigation is specifically carried out on an SAH measuring 120 cm in length, 85 cm in width, and 12 cm in height, which is oriented southward and inclined at a 30° angle. The results indicate that the improved SAH can exhibit a significant enhancement in performance, achieving an overall efficiency of 38.4%. Additionally, the modified SAH has the potential to increase air temperature by up to 28.9 °C at the specified tilt angle of 30°. Furthermore, the findings suggest that increasing the absorber area is an effective strategy to enhance the performance of the SAH. Such advancements in solar thermal collector efficiency are pivotal for accelerating the adoption of renewable energy in the industrial sector, contributing directly to the decarbonization of process heat and advancing the objectives of SDG 7 (Affordable and Clean Energy) and SDG 9 (Industry, Innovation, and Infrastructure).

Cite this article: Resen, I. S., Skheel, O. Raad, Al-Obaidi, M. A., Al-Musawi, S. S. and Hydrose, A. (2025). Augmentation of Solar Air Heater Performance by Experimental Modification. Journal of Solar Energy Research, 10(3), 2491-2500. doi: 10.22059/jser.2025.402707.1639

DOI: 10.22059/jser.2025.402707.1639



©The Author(s). Publisher: University of Tehran Press.

^aIraqi Ministry of Education, General Directorate Vocational Education, Iraq.

^bTechnical Instructors Training Institute, Middle Technical University, Baghdad, Iraq.

^cCollege of Engineering, Al-Naji University, Baghdad, Iraq.

^dCollege of Engineering, Gulf University, Sanad, 26489, Kingdom of Bahrain.

^{*}Corresponding Author Email:dr.mudhar.alaubedy@mtu.edu.iq

1. Introduction

Solar energy was regarded as a significant alternative to meet the ever-increasing energy demand [1,2]. Among numerous alternatives, solar energy emerges as the optimal resource to meet the growing energy demand. The conversion of solar energy into thermal energy is more advantageous than its direct utilisation [3-5]. The Solar air heater (SAH) is regarded as another of the most efficient systems among the several alternatives for harnessing solar energy for heating purposes across multiple sectors [6]. Also, it is a fundamental solar thermal energy technology designed to provide safe, clean, and durable hot air, applicable in various contexts, including agricultural drying. Natural ventilation can be utilised in both building space ventilation and industrial applications [7,8].

The efficiency of a SAH depends mainly on the heat transfer rate from its absorbing surface to the air. Indeed, the limited absorber area restricts the effectiveness of conventional SAHs. Therefore, several studies have focused on enhancing heat transfer area in SAHs. For instance, Karwa [9] conducted an experimental work to enhance the thermal efficiency (TE) of a SAH with an absorbent plate that featured longitudinally angled fins, creating many equilateral triangle airflow channels. It was found that a 2 m collector length with aluminium fins and a 26.5 mm triangular passage width can potentially boost TE by up to 25.8 %. Also, the researcher indicated that this design can improve heat transmission without increasing pumping power, surpassing that of conventional SAHs. Chabane et al. [10] investigated the effects of hexagonal barriers on heat transfer and pressure loss in an SAH. The researchers aimed to enhance the TE of SAH while minimising drop in pressure. Various setups with differing quantities of barriers were evaluated. The configuration, including 18 barriers, attained a maximum TE of 70%, followed by 14 baffles at 65%, 10 baffles at 65%, six barriers at 58%, and three baffles at 50%. Furthermore, the placement of six barriers at the middle of the SAH demonstrated an optimal performance, achieving a balance between elevated thermal efficiency and acceptable pressure drop.

Salah et al. [11] examined a trapezoid SAH in winter, contrasting with both natural and induced convection. Aluminium fins attached to both sides of the absorber improved heat transfer. The findings revealed that natural convection can achieve a TE of 73.5%, whereas forced convection attained 65%. The largest temperature disparity was 45.5 °C for

natural convection and 17 °C for forced convection. In addition, the researchers indicated that natural convection is more effective for applications requiring significant temperature differentials, but forced convection is preferable for residential heating purposes. A combination of staggered ribs and multi-gap V-down ribs was the subject of an experimental study by Deo et al. [12] on an SAH. According to the results, the ideal improvement was attained using a 60° angle of attack, a surface sharpness depth of 0.044, and an equivalent sharpness pitch of 12. Ventral collapse and rib staggers increased the TE metric by 2.44 times. That is why, under certain geometrical circumstances, openings in rib roughness are so effective.

According to Jin et al. [13], SAHs with several V-shaped ribs significantly outperform those with inline arrangements. This is because the former are better at generating subsidiary vortices and redeveloping flows. The researchers demonstrated that staggered rows of V-shaped ribs can optimise TE in SAHs, reaching a high thermo-hydraulic efficiency coefficient of 2.34. Gout et al. [14] studied SAH absorbers made from recycled aluminium cans and metal mesh, testing three configurations: vertical, vertical with meshes, and horizontal placement of containers. The findings indicated that the TE of 62.4% can be achieved for horizontal configuration TE. In contrast, the vertically packed cans and the vertically organized cans with meshes recorded efficiencies of only 40.7% and 45.8%, respectively, at a velocity of 0.043 kg/s m^2 .

Using ANSYS FLUENT, Shayan et al. [15] examined the impact of an artificially created pattern on thermo-hydraulic roughness the performance of SAHs with S-shaped absorber plates in either an inline or staggered arrangement. Specifically, the researchers maintained a constant conduit length of 30 mm and varied the fin pitch, which is the length of the axis between two succeeding S-shaped fins, from 5 to 20 cm. They tested four different pitch-to-height ratios: 1.667, 3.33, 5, and 6.667. Accordingly, they found that the most efficient way to improve the transfer of heat was to use a staggered, artificially rough design. Hedau et al. [16] developed a 3-D computational model to evaluate the hydrodynamic efficiency of the dual-pass SAH, utilising perforation barriers as turbulence-generating geometries and cylindrical phase change material (PCM) tubes. The researchers examined various parameters, including the tube diameter ratio (ranging from 0.2 to 0.51), the barrier width-to-height ratio (from 0.4 to 0.8),

and Reynolds numbers between 3000 and 13,100. The results indicated that the use of PCM can improve the ability of the absorbent surface to store heat at various Reynolds number.

Studying the effects of rough surfaces on a SAH absorber plate, Prassad et al. [17] use computational technique to identify and validate the optimal channel. A detailed analysis of the effects of a rectangular groove on exergetic ratio, pressure transmission, drop, and enhancement factor (TEF) was provided. Optimal parameters in terms of TEF also tend to have a high exegetics ratio. At a Reynolds number of 17100, the maximum TEF was achieved at proportional size 0.020, relative pitch 0.0667, and relative height 0.30, with an energetic ratio of 0.9949. Sharma et al. [18] enhanced the performance of SAH by incorporating six baffles with various configurations (i.e., diagonal, oblique diagonal, dimple with sloping dimple, curve, and sine waveform) through computational technique. The researchers examined the thermal and hydraulic efficiency (THP) at various Reynolds number, along with the Nusselt number, as well as friction factor. demonstrated that the placement and configuration of the baffle regularly influence the THP of the SAH, and the better TE was achieved for sine wave configuration at Re of 15500.

The ongoing advancement of SAH stems from its diverse applications and the suboptimal efficiency of the flat plate for heat transfer. As a result, the scholars have increasingly focused on continuous modifications to the absorber plate. Most of the studies mentioned focused on issues such as simplicity and efficiency of design, as well as the availability and cost of materials for a variety of industrial and residential air heating applications. The impact of the alterations to the absorbent surface was not entirely evident, despite numerous attempts to enhance the absorber plate's efficiency through surface alterations. Additionally, most research has concentrated solely on enhancing the performance of the absorption plate, overlooking operational aspects of the SAH, particularly the optimal inclination angle that maximizes potential efficiency based on the testing location. The current experimental study focused on the design and evaluation of an aluminum absorption panel, featuring rectangular pipes arranged in a linear configuration, conducted in the climate of Iraq. The primary aim of this technique is to offer an expanded surface area for heat exchange while maintaining a consistent SAH size for optimal efficiency.

2. Materials and Methods

2.1 Description of Experimental Work

The objective of the experimental work is to assess the impact of rectangular pipe absorber plates on the SAH's performance. The outdoor experiments were conducted in Wasit City, Iraq, situated at 44.36° east longitude and 32.43° north latitude, with the rig oriented southward at an inclined angle. Figure 1 presents both isometric and lateral views of the SAH. To minimise heat loss, the absorber plate was insulated from the rear. The following sections detail the system and its key components.

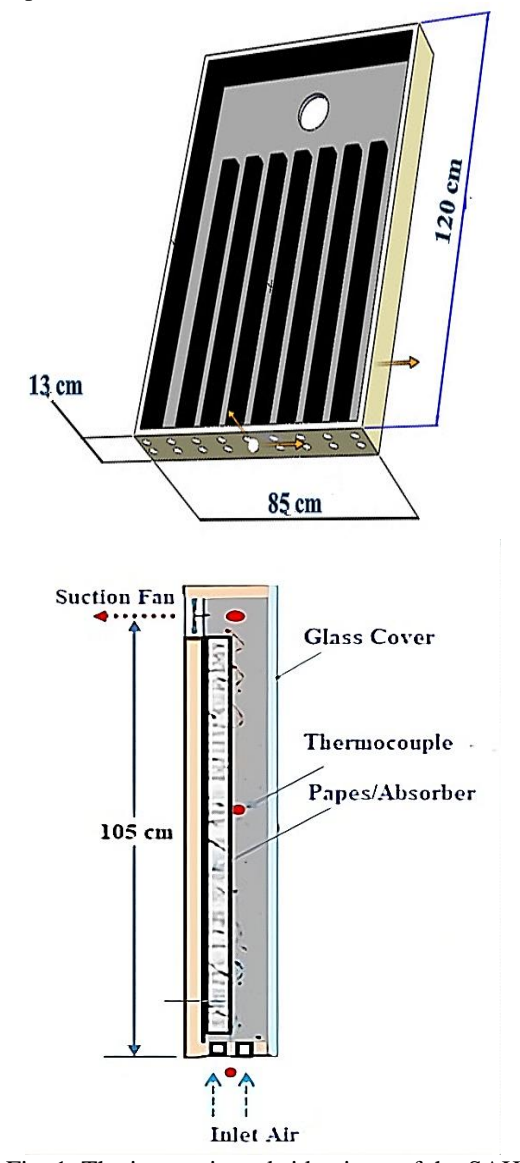


Fig. 1. The isometric and side views of the SAH system

2.1.1. The Absorber Plate

The current plate is constructed from commercial aluminium, utilising rectangular pipe produced by SAH and arranged in an array (Figure 2). Each pipe has a cross-section measuring 5 cm by 5 cm and a thickness of 0.08 cm. The intervening spaces between the pipes are 5 cm wide. Aluminium was used for the pipes because of its superior heat conductivity (k=237 W/m.K), which is roughly fourfold more than galvanized steel. Additionally, aluminium is lightweight and more cost-effective. The pipes enhance the exchange surface area, capture dispersed radiation at their surface [19], and function as conduits to circulate air, thereby increasing the heat transfer from their surface to the air within SAH. The surface of the plate wall is painted matte black to effectively absorb solar energy. The absorber plate has a thickness of 0.1 cm, a height of 100 cm, and a width of 84 cm.



Fig. 2. Rectangle pipes absorber plate

2.1.2. The Glass Cover

A glass sheet measuring 85 cm \times 120 cm \times 0.4 cm covers the current SAH, permitting sunlight ingress while confining long-wavelength rays to establish a greenhouse effect. Its low reflectivity and high light transmittance make the glass an ideal material for the transparent cover. This cover not only mechanically stabilizes the SAH but also protects it from the chilling effects of humidity and external influences.

2.1.3. The Insulation

The rear surface of the absorbing plate was insulated to minimise heat losses. A layer of glass

wool insulation, measuring 5 cm in thickness, was utilised and encased in aluminium foil.

2.1.4. Fan

A 20 CFM, 1.7-W DC fan was used to draw out the hot air. This fan was installed on the backside of the SAH, nearest the top part. To ensure unimpeded airflow, the fan diameter was adjusted to match that of the suction opening, eliminating the need for expansion joints.

2.2 Experiment Setup

The SAH was manufactured a wooden frame with a thickness of 3 cm and inside dimensions of 120 cm in length, 85 cm in breadth, and 12 cm in height. The wooden wall of SAH was secured with screws and double-sided foam tape. The SAH's length was greater than its width to ensure uniform thermal behavior and proportional airflow. Figure 3 illustrates the actual photograph of the experimental configuration, wherein the SAH was oriented southward and inclined at an angle of 30°. The absorber plates and pipes are coated with a black selective material to increase their ability to absorb solar radiation. The research was conducted from the period of 9 am to 6 pm on sunny days in September 2025. Figure 4 depicts the primary stages involved in the fabrication of the SAH with a rectangular pipe absorber plate.



Fig.3. Test rig



Fig. 4A. Manufacturing of the SAH.

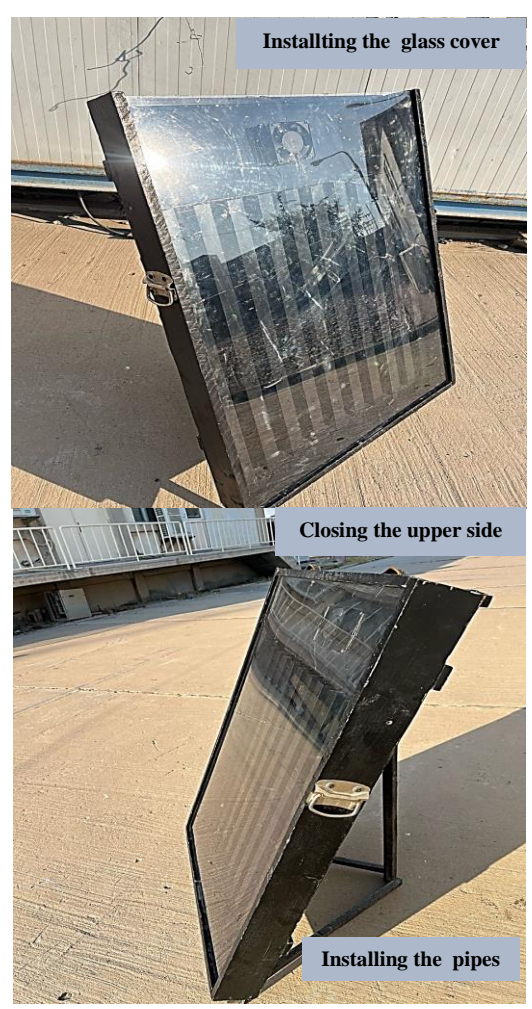


Fig. 4B. Manufacturing of the SAH.

2.3 Instrument Measurement

Five calibrated thermocouples of the K type were employed for measuring the temperature in the SAH, as depicted in Figure 5a. These thermocouples were installed at specific points, i.e. at the air inlet and outlet, on the absorbent surface, on the glass, and at the centre of the air gap. All thermocouple outputs were tracked utilising Ht-9815 data loggers, as illustrated in Figure 5b. The SM206E solar power meter monitored solar radiation intensity; it has a resolution of 0.1 W/m^2 and an error rate of $\pm 5\%$. This apparatus measured solar radiation incidence every 30 min perpendicular to the SAH. The air velocity at the output of the SAH was quantified using a GM8901 digital anemometer, which possesses a resolution of 0.1 m/s, a range of 0-30 m/s, and an accuracy of $\pm 3\%$ of its measurement.

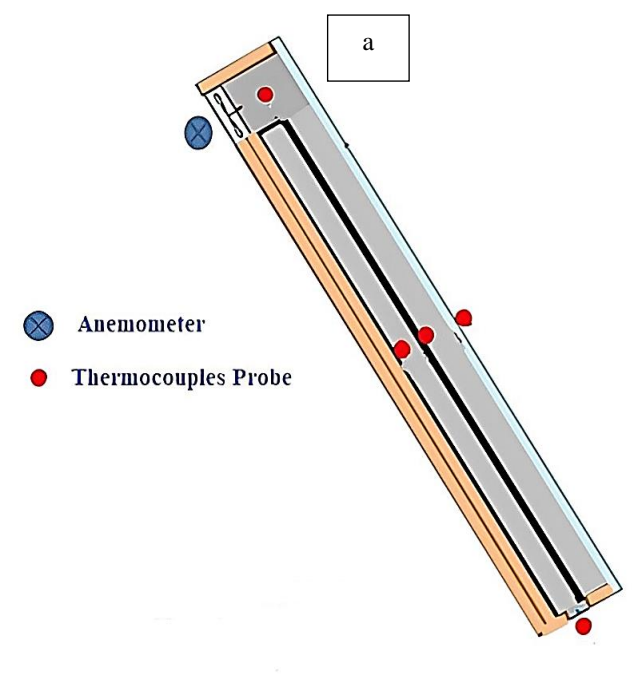




Fig.5. (a) Location of the thermocouple and (b) thermocouple thermometer

2.4 Data Reduction

The air volume flow rate was evaluated according to:

$$Q = VA \tag{1}$$

Q is volumetric flow rate. V and A are velocity and fan section area, respectively.

The useful heat energy of the air can be calculated in watts using the equation below [6]:

$$Q_{useful} = m C p_{,air} (T_{air,o} - T_{air,i})$$
 (2)
 m refers to the air flow rate, which is calculated as

the product of density and flow volume. T represents the temperature, while the subscripts air,o and air,i denote outgoing and incoming air, respectively.

Heat from solar radiation absorbed by the SAH is estimated using the following equation [20]:

$$Q_{abs} = \alpha \tau A_s I_t \tag{3}$$

 A_s denotes the surface area of the SAH (m²), τ signifies the glass transmittance at 0.96, α indicates the absorptivity of the pipes at 0.96, and I_t represents the radiation intensity measured (W/m²).

The SAH thermal efficiency is estimated using following equation [21]:

$$\eta_{th} = Q_{useful}/Q_{abs} \tag{4}$$

The overall thermal efficiency of the SAH can be calculated by the calculation based on the electrical consumption of the suction fan.

$$\eta_o = (Q_{useful} - P_{fan})/(\beta Q_{abs})$$
(5)

 β is the factor associated with the transformation of electricity into energy, valued at 0.2 [22], while P_{fan} represents the fan capacity measured (W).

3. Results and Discussion

The experimental results are exhibited, analyzed and discussed in the context of this section. The performance of an SAH with a rectangular pipe absorber plate was experimentally studied to evaluate how increasing the absorber area affects its efficiency. The thermal behavior of the SAH is assessed by establishing the air temperature and thermal gain.

3.1 Climatic conditions

The intensity and duration of solar radiation, along with ambient temperature, are crucial factors influencing the effectiveness of SAHs. Figure 6 shows the radiation intensity throughout the day, measured parallel to the SAH. The illustration shows that radiation progressively increases from the start of the day, peaking at midday with values of 1050 W/m² and 863 W/m² under daytime conditions before diminishing until sunset. The daily averages of solar radiation are approximately 687 W/m² and 543 W/m². Figure 6 also depicts the variation in ambient temperature, which varies depending on the weather conditions on different days. The maximum recorded temperatures ranging from 26.3 °C to 28.6 °C. The average temperatures range from 21.4 °C to 21.8 °C. Additionally, Figure 6 highlights the

proximity of ambient temperatures for the two days, facilitating a comparison of the SAH's performance on different days [23].

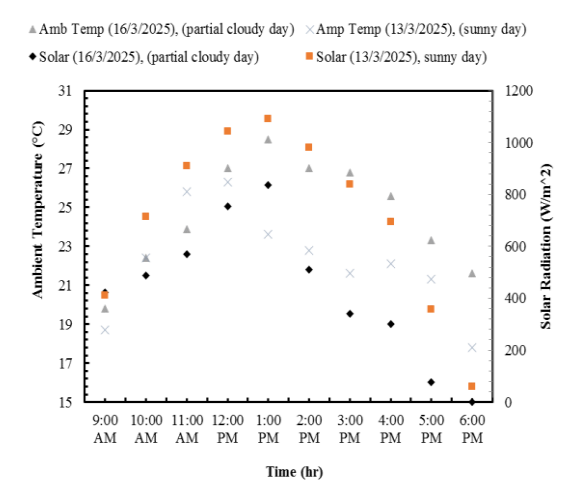


Fig. 6. Daytime ambient temperature and solar radiation variation

3.2 Temperatures within SAH

Raising the air temperature produced is the primary objective of any SAH, as this temperature is used to assess the efficiency of the SAH. Therefore, it is essential to examine how the inlet temperature affects SAH hot air outlet temperature and how temperatures vary at different locations within the heater, such as the absorber and the glass [24]. Figures 7 and 8, which update every half hour, illustrate the temperature distribution within the SAH on various days. Figures 7 and 8 show that, similar to solar radiation, the SAH's glass, absorber/pipes, and air gradually heat up from early hours until noon and then slowly decline until sunset.

The basic idea behind an SAH is that when sunlight hits a heater, it goes through a glass pane and into an absorber, which then becomes hotter. Accordingly, the air that is traveling through the absorber becomes further hotter as it comes into contact with its surface. Then, the absorber, pipes, hot air, and glass reach their maximum temperatures during the SAH in accordance with the air heater's thermal balance.

On a sunny day in March (March 13, 2025), as shown in Figure 7, the temperature of the absorber fluctuates between 53.5 °C and 81.3 °C. The temperature of the absorber is directly influenced by incident solar radiation. In the afternoon, solar

radiation also led to a decline in the temperature of the absorber wall. As a result, the temperature differential between the intake and output decreased. On the partially cloudy day of March 16, 2025, illustrated in Figure 8, the impact of cloud cover was apparent, as evidenced by the lower temperature values. The maximum temperature of the absorber wall reached 76 °C at approximately 1:10 PM, which can be attributed to the reduced solar radiation.

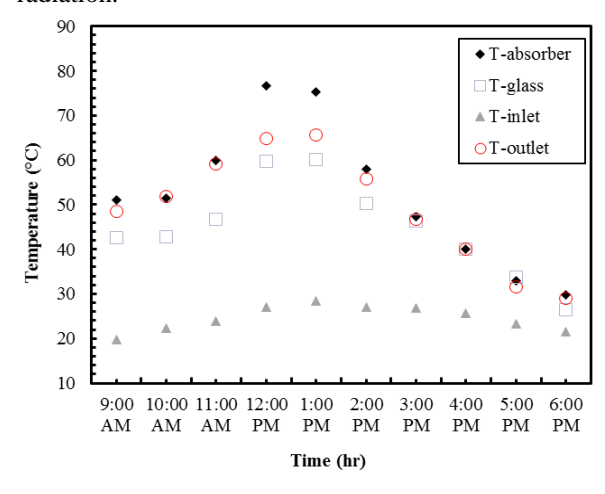


Fig. 7. Temperature variation of inlet and outlet air, glass, and absorber plate for a sunny day (13-3-2025)

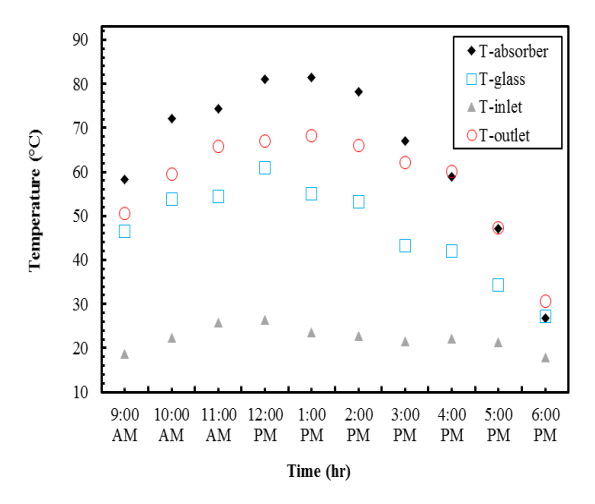


Fig. 8. Temperature variation of inlet and outlet air, glass, and absorber plate for a partial cloudy day (16-3-2025)

3.3 SAH Energy Analysis

The useful heat energy of the air obtained from the SAH was estimated using Eq. 2, and its temporal change is illustrated in Figure 9. Figure 9 distinctly illustrates that thermal power is minimal at the day's onset, progressively escalating to its zenith at noon, thereafter declining until sunset, mirroring the trend of solar radiation. The illustration indicates heat gain on a sunny day (March 13, 2025). The thermal gain reaches 391.5 W/m² at noon, even though it averages 184.3 W/m² during the day. Additionally, Figure 9 illustrates the performance of SAH under diminished sun energy [25,26]. Solar radiation intensity has a direct impact on thermal gain. The impact of cloudiness was noted as a decrease in thermal gain values on March 16, 2025. The heat gain of the SAH diminishes during the day, attaining 24.6 W at midday and averaging 162.8 W.

Figure 10 depicts the energy efficiency of the SAH and its temporal fluctuations across several days, as determined by Eq. 4. The illustration indicates that TE mirrors the solar radiation pattern, commencing at a low level, peaking at noon, and subsequently declining until nightfall. The solar air heater on a sunny day exhibits an average TE of 28.2%. The proposed SAH utilizes a fan that operates at roughly 1.7 W, allowing for the calculation of the SAH's overall TE at different conditions using Eq. 5, as illustrated in Figure 11. The proposed SAH utilises a minimal quantity of DC electrical energy, leading to a slight reduction in overall efficiency relative to usable energy efficiency efficiency. The overall of rectangular pipes rose to 38.4% at peak period, in comparison to a daily average TE of 27.6%.

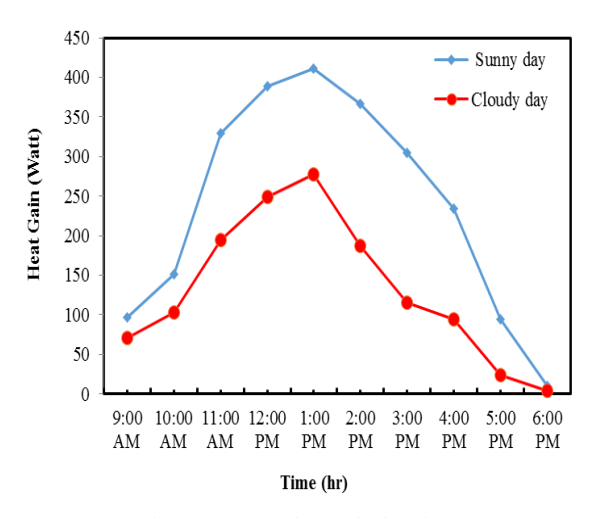


Fig. 9. Heat gain variation in SAH

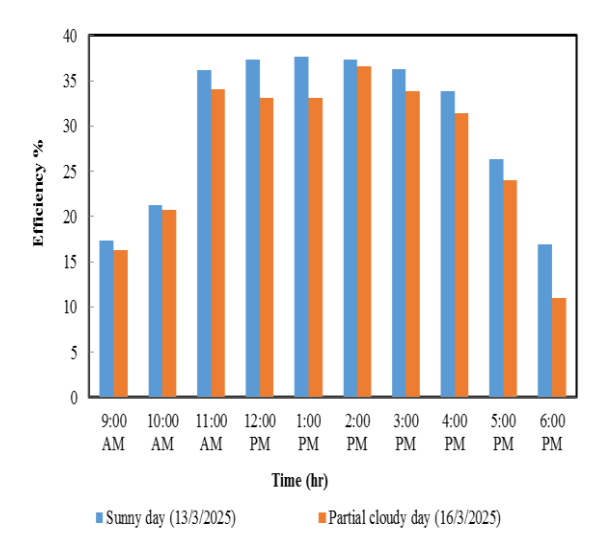


Fig. 10. Variation of efficiency of SAH

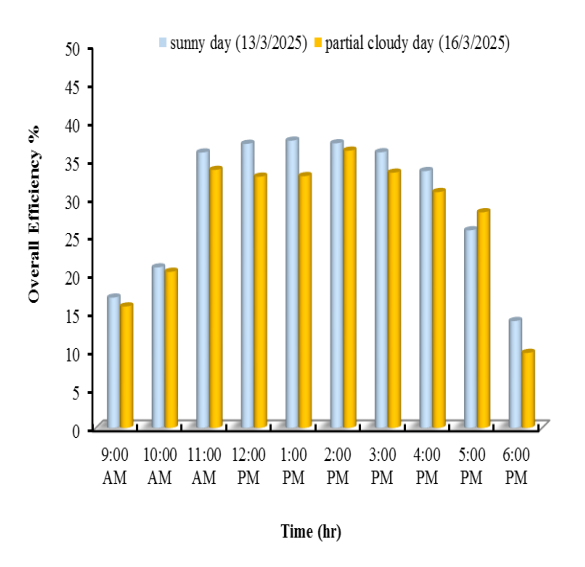


Fig. 11. Overall efficiency variation of SAH

4. Conclusions

This experimental investigation introduced a novel design for SAH utilising rectangular pipe absorber plates, aimed at enhancing the surface area to improve comprehensive efficacy of the SAH. The thermal behavior of the SAH is assessed by establishing the air temperature and thermal gain. The primary conclusions are as follows:

- 1. The modified SAH exhibited a significant improvement in performance
- 2. The suggested SAH can elevate air temperature by as much as 28.9 °C at a tilt angle of 30°.
- 3. A comprehensive efficacy of 38% was achieved at peak period, while the daily average efficacy during the experiment was 27.6%, due to the implementation of the proposed SAH.
- 4. In a partial cloudy day, the proposed SAH gives an acceptable overall efficiency.

Nomenclature	
A	Fan section area
A_s	Surface area of SAH
$C_{p, air}$	Specific heat capacity of air
I_t	Solar radiation intensity
m	Mass flow rate of air
PCM	Phase Change Material
P_{fan}	Fan capacity
Q	Volumetric flow rate
Q_{abs}	Absorbed solar heat energy
Quseful	Useful heat gain
SAH	Solar Air Heater
T	Temperature
T_{air}	Inlet air temperature
Tair, o	Outlet air temperature
V	Velocity
α	Absorptivity of the pipes
η_o	Overall thermal efficiency
η_{th}	SAH thermal efficiency
τ	Transmittance of the glass cover
Ψ	Electricity-to-energy conversion factor

References

[1] Rashid, F.L., Al-Obaidi, M.A., Hussein, A.K., Akkurt, N., Ali, B. and Younis, O., 2022. Floating solar stills and floating solar-driven membranes: Recent advances and overview of designs, performance and modern combinations. Solar Energy, 247, pp.355-372. https://doi.org/10.1016/j.solener.2022.10.044

- [2] Rashid, F.L., Al-Obaidi, M.A., Mahdi, A.J. and Ameen, A., 2024. Advancements in Fresnel lens technology across diverse solar energy applications: A comprehensive review. Energies, 17(3), p.569. https://doi.org/10.3390/en17030569
- [3] Resen, I.S., Alsayah, A.M., Alshukri, M.J., Eidan, A.A., Ali, S., Faraj, J. and Khaled, M., 2025. Exergy analysis of the effects of extreme hot conditions on cooling system efficiency: A case study of a split air conditioner. Case Studies in Chemical and Environmental Engineering, 11, p.101187.

https://doi.org/10.1016/j.cscee.2025.101187

- [4] Ali, M.F.M., Resen, I.S. and Ibrahim, I.J., 2023. Capillary Tube Length and Heat Transfer Dynamics in Air Conditioners: A Comparative Analysis of R-12 and Its Alternatives. International Journal of Heat and Technology, 41(6). https://doi.org/10.18280/ijht.410619
- [5] Hai, T., Mansir, I.B., Alshuraiaan, B., Abed, A.M., Ali, H.E., Dahari, M. and Albalawi, H., 2023. Numerical investigation on the performance of a solar air heater using inclined impinging jets on absorber plate with parallel and crossing orientation of nozzles. Case Studies in Thermal Engineering, 45, p.102913.
- [6] Alsibiani, S.A., 2024. Application of pulsating jet concept for efficiency improvement of solar-based air heaters. Cleaner Engineering and Technology, 18, p.100727. https://doi.org/10.1016/j.clet.2024.100727

https://doi.org/10.1016/j.csite.2023.102913

- [7] Resen, I.S. and Allawi, A.S., 2025, May. Thermal analysis of ventilated roof panels with PCM for insulation building roofs under extremely hot climate. In AIP Conference Proceedings (Vol. 3211, No. 1, p. 040009). AIP Publishing LLC. https://doi.org/10.1063/5.0257168
- [8] R.S. Gill, V.S. Hans, S. Singh, Investigations on thermo-hydraulic performance of broken arc rib in a rectangular duct of solar air heater, Int. Commun. Heat Mass Tran. 88 (2017) 20–27. https://doi.org/10.1016/j.icheatmasstransfer.2017.07.024
- [9] Karwa, R., 2024. Performance of finned absorber plate solar air heater having multiple triangular air flow passages in parallel under transition to turbulent flow condition. J. Sol. Energy Eng. 146, 1–46. https://doi.org/10.1115/1.4063494
- [10] CHABANE, F., Kherroubi, D., Arif, A., Moummi, N., Brima, A., 2020. Influence of the rectangular baffle on heat transfer and pressure drop in the solar collector. Energy Sources, Part A

- Recover. Util. Environ. Eff. 1–17. https://doi.org/10.1080/ 15567036.2020.1767727 [11] Salih, M.M.M., Alomar, O.R., Ali, F.A., Abd, H.M., 2019. An experimental investigation of a double pass solar air heater performance: a comparison between natural and forced air circulation processes. Sol. Energy 193, 184–194. https://doi.org/10.1016/j. solener.2019.09.060
- [12] Deo, N.S., Chander, S., Saini, J.S., 2016. Performance analysis of solar air heater duct roughened with multigap V-down ribs combined with staggered ribs. Renew. Energy 91, 484–500. https://doi.org/10.1016/j.renene.2016.01.067
- [13] Jin, D., Zuo, J., Quan, S., Xu, S., Gao, H., 2017. Thermohydraulic performance of solar air heater with staggered multiple V-shaped ribs on the absorber plate. Energy 127, 68–77. https://doi.org/10.1016/j.energy.2017.03.101
- [14] Guo, L., Nowzari, R., Saygin, H., Al-Bahrani, M., Nejad, M.G. and Baghaei, S., 2023. Experimental investigation and two-factor factorial analysis of a solar air heater with scrap wire meshes and cans as energy storage components. Journal of Energy Storage, 70, p.107998. https://doi.org/10.1016/j.est.2023.107998
- [15] Shayan, M.E., Ghasemzadeh, F. and Rouhani, S.H., 2023. Energy storage concentrates on solar air heaters with artificial S-shaped irregularity on the absorber plate. Journal of Energy Storage, 74, p.109289. https://doi.org/10.1016/j.est.2023.109289 [16] Hedau, A. and Singal, S.K., 2024. Thermohydraulic performance investigation of double pass solar air heater integrated with PCM-based thermal energy storage. Journal of Energy Storage, 79, p.110202. https://doi.org/10.1016/j.est.2023.110202 [17] Prasad, J.S., Datta, A. and Mondal, S., 2024. Flow and thermal behavior of solar air heater with grooved roughness. Renewable Energy, 220, p.119698. https://doi.org/ 10.1016/j.renene.2023.119698
- [18] Sharma, S., Das, R.K. and Kulkarni, K., 2021. Computational and experimental assessment of solar air heater roughened with six different baffles. Case Studies in Thermal Engineering, 27, p.101350. https://doi.org/10.1016/j.csite.2021.101350
- [19] Resen, I.S. and Allawi, A.S., 2024, August. Numerical study of lightweight panels incorporated with PCM used for insulation building roof under Iraqi climate. In AIP Conference Proceedings (Vol. 3105, No. 1, p. 030009). AIP Publishing LLC. https://doi.org/10.1063/5.0212340
- [20] Duffie, J. A., and Beckman, W. A. (1991). Solar Engineering of Thermal Processes. John Wiley and Sons.

- [21] Resen, I.S., Alsayah, A.M., Ali, M.F.M., Khudhur, D.S. and Singh, N.K., 2025, June. Designing Photovoltaic and Solar Water Heating Systems for Energy Efficiency and Environmental Sustainability in Iraq. In IOP Conference Series: Earth and Environmental Science (Vol. 1507, No. 1, 012015). IOP Publishing. https://doi.org/10.1088/1755-1315/1507/1/012015 [22] Alsibiani, S.A., 2023. Employment of roughened absorber palate and jet nozzles with different hole shapes for performance boost of solarair-heaters. Cleaner Engineering and Technology, p.100703. 17, https://doi.org/10.1016/j.clet.2023.100703
- [23] Al-khafaji, O.R. and Alabbas, A.H., 2020, February. Computational fluid dynamics modeling study for the thermal performance of the pin fins under different parameters. In IOP Conference Series: Materials Science and Engineering (Vol. 745, No. 1, p. 012070). IOP Publishing.
- [24] Alaskaree, È.H., Skheel Alkhafaji, O.R. and Al-Muhsen, N.F., 2020. Effect of chromium trioxide coating on the thermal performance of solar thermal collector. Karbala International Journal of Modern Science, 6(1), p.4.
- [25] Skheel Alkhafaji, O.R., 2019. The improvement of the solar air heater duct by wired ribs utilization. Karbala International Journal of Modern Science, 5(3), p.6.
- [26] Alkhafaj, O.R., Yasin, N.J. and Al-abbas, A.H., 2023. Optimization of wickless heat pipe heat exchanger using R1234-yf and ethanol as working fluids. Int. J. Appl. Sci. Eng, 20(3), pp.1-12.